

# VERIFICATION OF CONSTRAINED SHUTTLE PAYLOADS USING FREE-FREE MODAL TEST DATA: MATHEMATICAL BASIS

Chia-Yen Peng & Kenneth S. Smith

Applied Mechanics Technologies Section  
Structures & Dynamics Research Group  
Jet Propulsion Laboratory  
California Institute of Technology  
Pasadena, CA 91109, USA

## ABSTRACT

TO validate flight loads predictions, a modal test is required to verify the structural dynamic model of a spacecraft used in loads analyses. Traditionally, modal testing of shuttle payloads is performed with the payload in its fixed-base configuration, i.e., constraining all the payload/orbiter interface degrees of freedom. Practically, the fixed boundary conditions are quite difficult to achieve with large and massive payloads, such as the Shuttle Imaging Radar-C. This leads to the consideration of testing payloads in a free-free configuration, or other alternatives. In this paper, it will be shown analytically how free-free modes and residual flexibility data can be adequate to characterize the significant fixed-base modes. As a result, the fixed-base modes can be verified indirectly from the measurements of free-free modes and residual flexibility.

## NOMENCLATURE

$M_{gg}$	physical mass matrix
$K_{gg}$	physical stiffness matrix
$\omega_s$	natural frequencies of fixed-base modes
$\Psi'_{gs}$	mass-normalized fixed-base modes shapes
$\omega_f$	natural frequencies of free-free modes
$\Phi'_{gf}$	mass-normalized free-free modes shapes
$I_{ff}, I_{ss}$	identity matrix
$I'_{fs}$	cross-orthogonality
$p_f$	generalized coordinates of free-free modes
$q_i$	generalized coordinates of residual flexibility
$m_{ii}$	generalized mass of residual flexibility
$R_{ii}$	residual flexibility shapes
$f_i$	forces at interface degrees of freedom
$\hat{M}_{ff}$	constrained mass matrix
$\hat{K}_{ff}$	constrained stiffness matrix
$x_p$	all physical coordinates of model

## 1. INTRODUCTION

To validate flight loads predictions, the fidelity of a payload's structural dynamic model used in computing ascent and landing loads needs to be verified. The verification process requires a modal survey test of the physical structure and subsequent model correlation with test data.

Traditionally, modal testing of a shuttle payload is performed with the payload in its fixed-base configuration, i.e., constraining all the payload/orbiter interface degrees of freedom. To properly achieve this set of boundary conditions, the payload will be supported on a rigid fixture which has no modes in the frequency range of interest. The fixture must be fixed to a reinforced floor for which deformations do not interfere with the payload modes. Also, the payload/fixture interface has to be identical, or similar, to the payload/orbiter interface. No gap or friction is allowed since these will introduce amplitude dependent non-linearity.

Practically, in many cases, it is not possible to conduct a truly fixed-base test due to coupling between the test article and the fixture, especially with large and massive payloads, such as the Shuttle Imaging Radar-C (SIR-C), in addition, it is often difficult to accurately simulate the actual boundary constraints, and the cost of designing and constructing the fixture may be prohibitive [1]. This leads to the consideration of alternative modal test methods, including testing shuttle payloads in a free-free configuration using the residual flexibility technique [2,3]. The residual flexibility approach has been treated analytically in considerable detail. However, its application as a test method is quite limited [4,5].

In a free-free test, besides measuring free-free modes, the

payload/orbiter interface region needs to be test-verified as well. This can be done by exciting directly each of the interface attach degrees of freedom and extracting residual flexibility mode shapes from the Frequency Response Functions measured. The purpose of the present paper is to show analytically how free-free modes and residual flexibility data can be adequate to characterize the significant fixed-base modes. As a result, the fixed-base modes can be verified indirectly from the measurements of free-free modes and residual flexibility.

There are two steps involved in our mathematical approach for verifying constrained modes using free-free modal test data. First, a set of target free-free modes is selected which will be correlated to test measurements. Second, a free-free reduced model, using only selected target modes and residual flexibility, is constrained mathematically to generate fixed-base modes. These derived fixed-base modes are then compared to those computed directly from the full finite element model. If the resulting fixed-base frequencies and mode shapes agree, the structural dynamic model is considered test-verified in its constrained configuration.

In the following sections, each step of the proposed mathematical approach is described in detail and the governing equations are discussed. The method is then applied to the pre-test model of the SIR-C payload. A comparison of the fixed-base modes derived from free-free "test" data and those from the full finite element model is also presented.

## 2. SELECTION OF TARGET FREE-FREE MODES

### 2.1 Mathematical Formulation

Consider a full finite element model, described by a physical mass matrix  $M_{gg}$  and a stiffness matrix  $K_{gg}$ . Assume that the interface degrees of freedom are not yet constrained.

There are two sets of mode shapes of interest to the present discussion. First, the free-free modes of the system, which we will denote  $\Phi_{gl}$ , form a square invertible matrix with the properties

$$\Phi_{lg} M_{gg} \Phi_{gl} = I_{ll}, \quad (1)$$

$$\Phi_{lg} K_{gg} \Phi_{gl} = \text{diag}(\omega_l^2). \quad (2)$$

Note that  $\Phi_{lg}$  denotes the transpose of  $\Phi_{gl}$ . The values  $\omega_l$  are the free-free natural frequencies of the structure. Second, the fixed-base modes of the system, which we will denote  $\Psi_{gs}$ , form a rectangular matrix which is zero at the interface degrees of freedom, and for which

$$\Psi'_{sg} M_{gg} \Psi_{gs} = I_{ss}, \quad (3)$$

$$\Psi'_{sg} K_{gg} \Psi_{gs} = \text{diag}(\omega_s^2). \quad (4)$$

The values  $\omega_s$  are the fixed-base natural frequencies of the structure. For both sets of modes, we assume the full set of modes, even though all of the modes are not usually computed.

Because the matrix  $\Phi_{gl}$  is square and invertible, it is possible to express any vector  $x_g$  as a linear combination of the columns of  $\Phi_{gl}$ . In particular, the fixed-base mode shapes can be written as

$$\Psi_{gs} = \Phi_{gl} \Gamma_{ks}, \quad (5)$$

for some matrix  $\Gamma_{ks}$ . In fact, we can find an expression for  $\Gamma_{ks}$  by premultiplying equation (5) by  $\Phi_{lg} M_{gg}$ , and using equation (1):

$$\Gamma_{ks} = \Phi_{lg} M_{gg} \Psi_{gs}. \quad (6)$$

Thus,  $\Gamma_{ks}$  is simply the cross-orthogonality product between the free-free and fixed-base modes of the structure. Since both sets of mode shapes are mass-normalized, clearly the values  $\Gamma_{ks}$  must lie between -1 and 1.

Referring back to equation (5), it can be seen that the relative size of each term of  $\Gamma_{ks}$  is an indication of the importance of free-free mode  $l$  in describing fixed-base mode  $s$ . Now premultiply equation (5) by  $\Psi'_{sg} M_{gg}$ , and use equations (3) and (6) to simplify:

$$I_{ss} = \Gamma'_{sl} \Gamma_{ks}. \quad (7)$$

Examining the diagonal terms of this equation, we see that the sum of the squares of the cross-orthogonality terms must equal unity; i.e., for fixed-base mode  $s$ ,

$$\sum_l \Gamma_{sl}^2 = 1. \quad (8)$$

Therefore, not only are the cross-orthogonality values indicators of the importance of free-free modes in representing the fixed-base modes, but the sum of the squares of the cross-orthogonality terms for a given fixed-base mode must be equal to 1. This is true only if all of the free-free modes are included in the sum. For any subset of the free-free modes, the sum will be something less than unity.

This mathematical exercise leads to an approach for determining target free-free modes. The cross-orthogonality matrix between free-free and fixed-base modes is first computed, then importance is assigned to each free-free mode based on its relative contribution to the sum in equation (8). For any selection of target free-free modes, the partial sum over those modes is an indication of the completeness of the set for describing any fixed-base mode.

## 2.2 Application to SIR-C

To illustrate the mathematical approach described above, the analysis performed to select a set of free-free target modes for the SIR-C structure, using the pre-test model, is described herein.

The cross-orthogonality matrix  $\Gamma_{ls}$  was computed for 188 fixed-base modes up to 90 Hz, and 195 free-free modes up to 90 Hz. For each of the first 20 fixed-base modes (identified as significant modes), the sum of equation (8) was computed step by step as each free-free mode was added to the sum. The results are plotted in Figures 1a (fixed-base modes 1-10) and 1b (modes 11-20). As predicted by the equation, the total approaches 1. Although it is not obvious from these figures, each of the first 28 free-free modes is significant to at least one of the first 20 fixed-base modes. Beginning with free-free mode number 29, the significance is much smaller. The one exception is free-free mode number 62, which is very significant for fixed-base mode 20 (circles on Figure 1b).

Based on this study, it was determined that the target free-free modes should be modes 1 through 28, and mode 62. Note that the first eleven free-free modes are rigid body or internal mechanism modes, and can be considered to have perfectly known mode shapes (determined only by geometry). Therefore, there are only 18 elastic target modes (modes 12 through 28 and mode 62).

In addition to the target free-free modes, the residual flexibility mode shapes will be measured as well using the Frequency Response Functions measured from direct excitation of each of the interface attach degrees of freedom. Each residual flexibility mode shape is a combination of all of the non-target free-free modes.

Figure 2 shows the total obtained in equation (8) when the sum is taken over all of the target free-free modes plus the residual flexibility modes. Each fixed-base mode has its own result, which is between 0 and 1. This figure shows that the first 20 fixed-base modes are indeed almost completely described by the target set. Figure 3 shows the same results, but plotted as a function of effective mass rather than mode number. This figure demonstrates that all of the modes with effective mass greater than approximately 3% of the total mass are well represented by the target set together with residual flexibility.

## 3. COMPARISON OF FIXED-BASE MODES

The orthogonality coefficient study described in the previous section is useful for developing the set of target free-free modes. The results do not conclusively demonstrate the adequacy of the target modes, however. This section describes the steps taken to show that the free-free model is equivalent to the fixed-base model.

### 3.1 Mathematical Formulation

It was shown that a reduced equation of motion can be written using low-frequency free-free modes and residual flexibility shapes. The reduced equation of motion in modal coordinates is:

$$\begin{bmatrix} \mathbf{I}_{ff} & \mathbf{0} \\ \mathbf{0} & \mathbf{m}_{ff} \end{bmatrix} \begin{Bmatrix} \ddot{\mathbf{p}}_f \\ \ddot{\mathbf{q}}_r \end{Bmatrix} + \begin{bmatrix} \text{diag}(\omega_f^2) & \mathbf{0} \\ \mathbf{0} & \mathbf{R}_{ff} \end{bmatrix} \begin{Bmatrix} \mathbf{p}_f \\ \mathbf{q}_r \end{Bmatrix} = \begin{Bmatrix} \Phi_{ff} \\ \mathbf{R}_{ff} \end{Bmatrix} \mathbf{f}_i, \quad (9)$$

where  $\mathbf{p}_f$  the generalized coordinates of free-free modes,  $\mathbf{q}_r$  the generalized coordinates of residual flexibility shapes,  $\omega_f$  the natural frequencies of free-free modes,  $\mathbf{f}_i$  the forces at interface degrees of freedom,  $\mathbf{I}_{ff}$  is an identity matrix,  $\mathbf{m}_{ff}$  the generalized mass of residual flexibility shapes,  $\mathbf{R}_{ff}$  the partition of the residual flexibility matrix  $\mathbf{R}_{fi}$  at the interface degrees of freedom,  $\Phi_{ff}$  the partition of the free-free modes  $\Phi_{fi}$  at the interface degrees of freedom.

Physical coordinates,  $\mathbf{x}_g$ , are then obtained from modal coordinates by the equation

$$\mathbf{x}_g = \begin{bmatrix} \Phi_{gl} & \mathbf{R}_{gi} \end{bmatrix} \begin{Bmatrix} \mathbf{p}_l \\ \mathbf{q}_i \end{Bmatrix}. \quad (10)$$

To establish a relationship between the free-free model and a fixed-base model, we will use equations (9) and (10) to predict fixed-base modes. From equation (10) we can express displacements at the interface degrees of freedom as

$$\mathbf{x}_i = \begin{bmatrix} \Phi_{il} & \mathbf{R}_{ii} \end{bmatrix} \begin{Bmatrix} \mathbf{p}_l \\ \mathbf{q}_i \end{Bmatrix}. \quad (11)$$

Constrain the interface by setting  $\mathbf{x}_i = \mathbf{0}$ . One way to enforce this constraint is by eliminating the residual flexibility coordinates. This requires

$$\mathbf{q}_i = -\mathbf{R}_{ii}^{-1} \Phi_{il} \mathbf{p}_l. \quad (12)$$

Substituting this equation into equation (9), we obtain the constrained equation of motion:

$$\hat{\mathbf{M}}_{ll} \ddot{\mathbf{p}}_l + \hat{\mathbf{K}}_{ll} \mathbf{p}_l = \mathbf{0}, \quad (13)$$

where

$$\hat{\mathbf{M}}_{ll} = \mathbf{I}_{ll} + \Phi_{il} \mathbf{R}_{ii}^{-1} \mathbf{m}_{ii} \mathbf{R}_{ii}^{-1} \Phi_{il}; \quad (14.1)$$

$$\hat{\mathbf{K}}_{ll} = \text{diag}(\omega_l^2) + \Phi_{il} \mathbf{R}_{ii}^{-1} \Phi_{il}. \quad (14.2)$$

These "constrained" mass and stiffness matrices are no longer diagonal. In the constrained model, physical displacements are obtained as

$$\mathbf{x}_g = \Phi_{gl} \mathbf{p}_l + \mathbf{R}_{gi} \mathbf{q}_i \quad (15)$$

$$= (\Phi_{gl} - \mathbf{R}_{gi} \mathbf{R}_{ii}^{-1} \Phi_{il}) \mathbf{p}_l. \quad (16)$$

The fixed-base mode shapes diagonalize the constrained mass and stiffness matrices. Let  $\varphi_{ls}$  be a square matrix for which

$$\varphi_{sl} \hat{\mathbf{M}}_{ll} \varphi_{ls} = \mathbf{I}_{ss}; \quad (17.1)$$

$$\varphi_{sl} \hat{\mathbf{K}}_{ll} \varphi_{ls} = \text{diag}(\omega_s^2). \quad (17.2)$$

This matrix is obtained by solving the eigenvalue problem for  $\hat{\mathbf{M}}_{ll}$  and  $\hat{\mathbf{K}}_{ll}$ . Then the fixed-base frequencies predicted by constraining the free-free model are  $\omega_s$ . Further, the predicted fixed-base mode shapes at physical degrees of freedom,  $\hat{\Psi}_{gs}$ , are obtained by applying equation (16):

$$\hat{\Psi}_{gs} = (\Phi_{gl} - \mathbf{R}_{gi} \mathbf{R}_{ii}^{-1} \Phi_{il}) \varphi_{ls}. \quad (18)$$

Note that the constrained mass and stiffness matrices depend only on the interface partition  $\mathbf{R}_{ii}$  of the residual flexibility matrix. The residual flexibility at other degrees of freedom in the model does not affect these matrices, and hence has no influence on the predicted fixed-base natural frequencies. The predicted mode shape, however, depends on the full residual flexibility shape, as seen in equation (18).

### 3.2 Application to SLR-C

The previously outlined approach was applied to the pre-test SLR-C model. The free-free model used all of the target free-free modes (modes 1-28 and mode 62), supplemented with the residual flexibility mode shapes for the twelve interface degrees of freedom.

The fixed-base modes computed from the free-free model were compared with the fixed-base modes computed from the full finite element model. The two sets of modes were compared in two ways. The natural frequencies are compared in Table 1. The table shows that for all of the significant fixed-base modes (i.e., modes 1 through 20), the frequencies agree within approximately 1%. Mode shape comparison is shown in Table 2, which shows cross-orthogonality between the fixed-base mode shapes computed from the full model, compared with those computed from the free-free modal model. The rows of Table 2 correspond to the modes of the full model, and the columns to the modes derived from the free-free modal model. With two exceptions, all of the off-diagonal terms in the first 20 modes are less than 10%. The exceptions are mode pairs 2 and 3 and 14 and 15, which show off-diagonal terms of 12% and 15% respectively. In each case, the pairs of modes have frequencies within a couple of percent, and the off-diagonal terms merely represent a small "rotation" of the mode pair. This is a common phenomenon with closely spaced modes, and does not invalidate the result. Note also that modes 19 and 20 traded places, but the

frequency shift is quite small.

Based on the above results, it is demonstrated that the selected target free-free modes plus residual flexibility will be sufficient to predict the first 20 fixed-base modes up to 25 Hz range.

#### 4. CONCLUSIONS

An analytical approach was developed to demonstrate the mathematical basis for verifying constrained modes using free-free modal test data. There are two steps involved in this approach. First, a set of target free-free modes is selected based on the cross-orthogonality matrix between free-free and fixed-base modes. For any selection of target free-free modes, the completeness of the set for describing any fixed-base mode is checked. Second, the free-free reduced analytical model, using only selected target modes and residual flexibility, is constrained mathematically to generate fixed-base modes. These derived fixed-base modes are then compared to those computed directly from the full finite element model.

This approach was applied to the pre-test model of the SIR-C shuttle payload. The results showed a good prediction of the first 20 fixed-base modes up to 25 Hz range using 29 target free-free modes plus 12 residual flexibility shapes. This indicates that the free-free modal representation of the structure is equivalent to the fixed-base representation of the model for the significant fixed-base modes up to 25 Hz range. So, by measuring and correlating the target free-free modes and residual flexibility, we should have a high degree of confidence in the fixed-base modes of the correlated model.

#### 5. ACKNOWLEDGMENT

The work described herein was conducted by the Jet Propulsion Laboratory, California Institute of Technology, under contract with National Aeronautics and Space Administration.

#### 6. REFERENCES

1. Admire, J.R., Tinker, M.L., and Ivey, E. W., "Mass-Additive Modal Test Method for Verification of constrained Structural Models," Proceedings of the 10th International Modal Analysis Conference, February 1992.
2. Blair, Mark A., "Space Station Module Prototype Alternative Modal Tests: Convergence to Fixed Base," Proceedings of the 11th International Modal Analysis Conference, February 1993.
3. Blair, Mark A., "Space Station Module Prototype Alternative Modal Tests: Fixed Base Alternatives," Proceedings of the 11th International Modal Analysis Conference, February 1993.
4. Brillhart, R.D., Hunt, D. L., Flanigan, C. C., Guinn, R., and Hull R., "Transfer Orbit Stage Modal Survey, Part 1, Measurement of Free-Free Modes and Residual Flexibility," Proceedings of the 7th International Modal Analysis Conference, February 1989.
5. Brillhart, R.D., Hunt, D. L., Flanigan, C. C., Guinn, R., and Hull R., "Transfer Orbit Stage Modal Survey, Part 2, Model Correlation," Proceedings of the 7th International Modal Analysis Conference, February 1989.
6. Smith, K. and Peng, C-Y., "SIR-C Antenna Mechanical System Modal Test and Model Correlation Report (Volume 1)," Internal Document JPL D-10694, April 21, 1993, Jet Propulsion Laboratory, California Institute of Technology, Pasadena, CA.



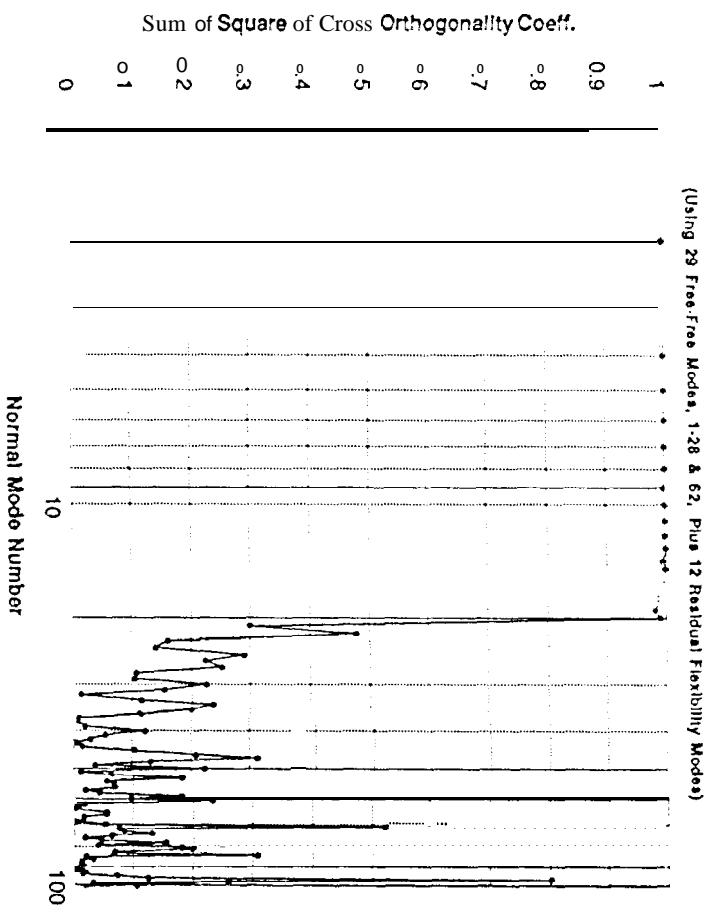


Figure 2. Sum of Orthogonality Coefficients Over Target & Residual Flexibility Modes

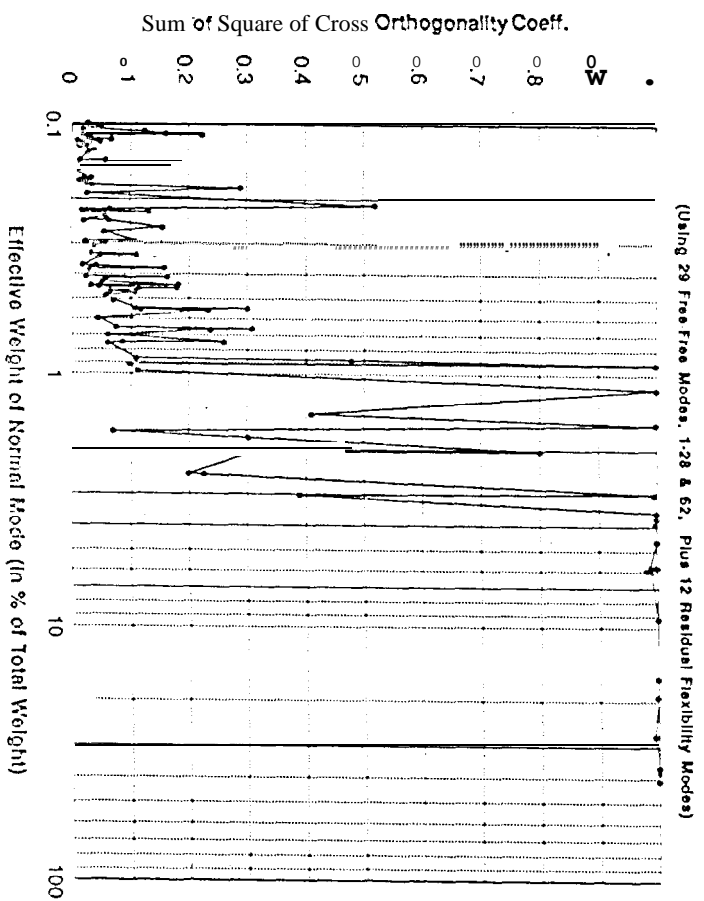


Figure 3. Sum of Orthogonality Coefficients vs. Ineffective Mass of Fixed-Base Modes

Mode #	Original	Derived*	Difference	Diff. in %
1	1227	12.27	-0.01	-0.05
2	1347	13.46	-0.01	-0.07
3	13.78	<b>13.65</b>	-0.13	<b>-0.96</b>
4	14.74	<b>14.63</b>	-0.11	-0.78
5	15.14	15.10	-0.04	-0.25
6	15.61	<b>15.58</b>	-0.03	-0.70
7	1653	16.39	-0.14	-0.84
8	17.92	17.91	-0.02	-0.09
9	<b>20.35</b>	20.37	0.03	0.14
10	20.76	20.79	0.02	0.12
11	21.88	21.89	0.01	<b>0.06</b>
12	22.58	22.58	0.00	0.02
13	2317	23.18	0.01	0.03
14	2372	23.82	0.09	0.40
15	<b>24.01</b>	24.04	0.03	0.12
16	24.29	24.34	0.04	0.18
17	2461	24.65	0.04	0.18
18	2586	25.56	-0.30	-1.15
19	2683	26.71	-0.12	-0.45
20	<b>27.08</b>	26.94	-0.14	<b>-0.52</b>
21	27.71	32.20	4.40	<b>16.17</b>
22	<b>28.14</b>	36.95	8.81	31.30
23	2873	3836	9.64	3355
24	2946	<b>50.17</b>	<b>20.71</b>	70.29
25	<b>30.77</b>	57.76	<b>26.99</b>	87.73
26	31.26	<b>58.51</b>	27.25	87.17
27	3178	<b>62.33</b>	30.55	<b>96.12</b>
28	3264	<b>66.74</b>	34.10	10448
29	3303	101.32	<b>68.29</b>	20678

\*: derived from .29 free-free/12 residual flexibility modes

Table 1. Comparison of Fixed-Base Mode Frequencies

	7	2	3	4	5	6	7	8	9	10	11	12	13	14	15	16	17	18	19	20	21	22	23	24	25	26	27	28	29
1	100																												
2		100																											
3			100																										
4				100																									
5					100																								
6						100																							
7							100																						
8								100																					
9									100																				
10										100																			
11											100																		
12												100																	
13													100																
14														100															
15															100														
16																100													
17																	100												
18																		100											
19																			100										
20																				100									
21																					100								
22																						100							
23																							100						
24																								100					
25																									100				
26																										100			
27																											100		
28																												100	
29																													100

Table 2. Cross Orthogonality of Full Model vs. Free-Free Modal Model  
Fixed-Base Mode Shapes